Article ID: 1006-8775(2024)02-0180-09

Analysis of Summer Cold Vortex Activity Anomalies in Northeastern China and Their Relationship with Regional Precipitation and Temperature

KONG Yang (孔 阳)[1], LU Chu-han (卢楚翰)[1,2], LI Kai-li (李凯丽)[3], SHEN Yi-chen (沈逸辰)[1]

(1. Key Laboratory of Meteorological Disaster, Ministry of Education, Nanjing University of Information Science and Technology, Nanjing 210044 China; 2. Key Laboratory of Ecosystem Carbon Source and Sink, China Meteorological Administration (ECSS-CMA), Wuxi University, Wuxi, Jiangsu 214063 China; 3. Nanjing Zhongke Huaxing Academy of Emergency Science and Technology, Nanjing 210032 China)

Abstract: The Northeastern China cold vortex (NCCV) is one type of strong cyclonic vortex that occurs near Northeastern China (NEC), and NCCV activities are typically accompanied by a series of hazardous weather. This paper employed an automatic algorithm to identify the NCCVs from 1979 to 2018 and analyzed their circulation patterns and climatic impacts by using the defined NCCV intensity index (NCCVI). The analysis revealed that the NCCV activities in summer exhibited a strong inter-annual variability, with an obvious periodicity of 3–4 years and 6–7 years, but without significant trends. In years when the NCCVI was high, NEC experienced negative geopotential height anomalies, cyclonic circulation, and cooler temperature anomalies, which were conducive to the maintenance and development of NCCV activities. Furthermore, large amounts of water vapor converged in NEC through two transportation routes as the NCCVs intensified, leading to a significant positive (negative) correlation with the summer precipitation (surface temperature) in NEC. The Atlantic sea surface temperature (SST) anomalies were closely related to summer NCCV activities. As the Atlantic SST rose, large amounts of surface sensible and latent heat flux were transported into the lower troposphere, inducing a positive geopotential height anomaly that occurred on the east side of the heat source. As a result, an eastward diverging flow was formed in the upper troposphere and propagated downstream, i.e., the eastward propagating Rossby wave train, which eventually led to a coupled circulation in the Ural Mountains and NEC, as well as more intensive NCCV activities in summer.

Key words: Northeastern China cold vortex (NCCV); anomaly; climatic effects; precipitation; surface temperature; development mechanisms

CLC number: P461 **Document code:** A

Citation: KONG Yang, LU Chu-han, LI Kai-li, et al. Analysis of Summer Cold Vortex Activity Anomalies in Northeastern China and Their Relationship with Regional Precipitation and Temperature [J]. Journal of Tropical Meteorology, 2024, 30 (2): 180–188, https://doi.org/10.3724/j.1006-8775.2024.016

1 INTRODUCTION

The Northeastern China cold vortex (NCCV) is a powerful cyclonic system that forms near Northeastern China and its vicinity, often bringing with it a deep and cold air mass. As a key player in the mid-latitude atmospheric circulation, the NCCV is associated with a range of severe weather events, including heavy rain, hail, thunderstorms, strong winds, and intense convection (Zhang et al. [1]), as well as low-temperature freezing (He et al. [2]). These weather patterns have a significant impact on agriculture and the socio-economic landscape of Northeastern China and East Asia, prompting extensive research into their major circulation features and climatic effects.

Typically spanning 500–1000 km in size, the NCCV has a life cycle of about 5–7 days (He et al. [3]; Hu et al. [4]). Previous studies have shown that the frequency of NCCV has obvious seasonal variations, peaking predominantly during the warm season (Hu et al. [4]; Nieto et al. [5]; Zhang et al. [6]; Awan et al. [7]). Correspondingly, cyclones in NEC occur more (less) frequently in summer (winter) (Wernli and Schwierz [8]; Lu [9]). Statistically, the Guliya Mountains and Heihe River are the main origins of the NCCV (Zhang et al. [6]; Sun et al. [10]; Xie et al. [11]). Liu et al. [12] observed a significant upward trend in the frequency and duration of NCCV activities between May and August.

The development of NCCV is closely related to the atmospheric circulation. Lian et al. [13] showed that the NCCV activities in early summer are related to the upstream blocking circulation in the Ural Mountains and the downstream anomalous circulation in the Northwestern Pacific. In the strong years of NCCV activities, a blocking circulation occurs in the vicinity of Ural Mountains by the synergistic effects of Rossby wave energy and transient eddy forcing, which is conducive to the maintenance and strengthening of NCCV activities. Liang et al. [14] pointed out that there is an obvious negative correlation between the NCCV and the Okhotsk blocking high in summer, and

Received 2023-09-26; **Revised** 2024-02-15; **Accepted** 2024-05-15

Funding: National Natural Science Foundation of China (41975073,42274215); Wuxi University Research Start-up Fund for Introduced Talents (2023r037); Qinglan Project of Jiangsu Province for DING Liu-guan; "333" Project of Jiangsu Province for DING Liu-guan

Biography: KONG Yang, Ph. D. candidate, primarily engaged in research on climate change.

Corresponding author: LU Chu-han, e-mail: luchuhan@nuist.edu.cn

the southwesterly flow on the east side of the NCCV provides favorable warm and wet conditions for the development of the Okhotsk blocking high, which in return limits the movement of NCCV and confines it in NEC for a long time. Liu et al. [15] found that the formation and development of NCCV are influenced by the cut-off low pressure (CL) in the upper troposphere, and when CL develops intensely, NCCV can stretch from the middle and upper troposphere to the lower troposphere, with a deep vertical structure and a cold core. The position of the western Pacific subtropical high (WPSH) also affects NCCV activities, i.e., when the position of WPSH shifts to the north, NCCV activities strengthen considerably (Sun et al. [10]). Moreover, Gao et al. [16] found that the lower sea surface temperature (SST) of Kuroshio in the early period is favorable for the enhancement of summer NCCV. Zhang et al. [17] proposed that the spring positive SST anomalies (SSTA) in the critical mid-latitude Atlantic region lead to an increased frequency of slowly developing cyclones in East Asia.

NCCV is the main synoptic system for precipitation in NEC, and its anomalous activity often leads to severe droughts or floods. For example, the summer of 1998 saw frequent NCCV activities, resulting in persistent and heavy precipitation along the Songhua and Nenjiang river basins (Zhang and Tao [18]; Zhao and Sun [19]). Therefore, previous studies have been done extensively on the NCCV and precipitation in East Asia (He et al. [3]; Hu et al. [4]). He et al. [3] found that there is a significant positive correlation between the NCCV and the rainfall of Meiyu, i.e., the Meiyu rainfall will be greater when NCCV activity is enhanced. Hu et al. [4] indicated that the summer precipitation in the Yangtze River Basin tends to increase significantly when NCCV activities are more active. Xie et al. [20] further pointed out that the NCCVs associated with the Ural Mountains and the Yakutsk-Okhotsk Sea are more likely to cause anomalously heavy precipitation in NEC. Moreover, the cooling effect caused by the persistent activity of NCCV is a major reason for the low temperature and freezing disasters (Ding [21]). When NEC is under the control of persistent NCCV activities, the northerly flow on the west side of NCCV transports cold air from high-latitude to the middle and low latitudes, which is likely to lead to low temperatures (Hu et al. [4]).

Many previous studies have investigated the characteristics of NCCV and its climatic effects (He et al. [2, 3]; Liu et al. [22]; Lu et al. [23]; Miao et al. [24]; Yang et al. [25]). However, their emphases have primarily been on quantifying the intensity of NCCV or studying its relationship with precipitation in East Asia. Further clarification is needed regarding the atmospheric circulation patterns at mid-to-high latitudes in the Northern Hemisphere. Based on previous results, this paper focused on the atmospheric circulation characteristics of synoptic NCCV in summer and further studies its climate effects and development mechanisms. Firstly, the study utilized the cyclone identification algorithm modified by Lu [9] to obtain the NCCV dataset during 1979–2018. Secondly, a composite intensity index was formulated for summer NCCVs based on their strength and the conditions in their peripheral areas within NEC. The paper then proceeded to analyze atmospheric circulation patterns in years with anomalous NCCV activity and explore their relationship with precipitation and temperature. Finally, the study examined the effect of SST in the Northern Hemisphere to further investigate the development mechanisms of NCCV.

2 DATA AND METHODS

2.1 *Data*

The data used in this paper included the ERA-Interim reanalysis dataset (ECMWF [26]; Dee et al. [27]) from the European Centre for Medium-Range Weather Forecasts. The geopotential height field at 850 hPa with T255 Gaussian grid (with a resolution of about 0.7°×0.7°) and 6 hours' interval from 1979 to 2018 was used to identify the NCCV. Monthly data for meteorological parameters, such as temperature, pressure, geopotential height, humidity, wind, and surface heat flux, were also used. The precipitation and temperature data of meteorological stations in China from 1979 to 2018 were derived from the China Meteorological Data Network. This data has been quality-controlled, and the data quality and completeness have been significantly improved relative to previously released products. SST data for the same period from Hadley Center with a resolution of 1°×1° (Hadley Centre Global Sea Ice and Sea Surface Temperature [28]) were also adopted.

2.2 *Methods of NCCV identification*

In this study, a cyclone identification algorithm modified by Lu [9] was used to identify summer (June–August) extratropical cyclones from 1979 to 2018. This algorithm is able to effectively track the extreme values of grids based on fields of different meteorological parameters (e.g., sea level pressure and geopotential height field) and search outward for peripheral closed contours at specific contour intervals. Finally, the extreme grid surrounded by the outer closed contours was considered as the center of the cyclone, and the area within its outermost closed contours was considered as the cyclone influence area. Moreover, Neu et al. [29] compared plenty of methods and found that different identification algorithms usually have uncertainties in identifying cyclones in high terrain; therefore, in order to mitigate the influence of terrain, the 850 hPa geopotential height field at 6 hours' interval was adopted in this paper.

After that, we determined NCCVs based on their influence area. Specifically, if the influence area of a cyclone falls into NEC (42°–55°N, 115°–130°E) at any time frame during its lifetime, it is considered an NCCV. Following this criterion, the composite characteristics of synoptic systems were fully considered, including the cases where the cyclone's center was not located in NEC,

but its peripheral area reached and impacted NEC. Furthermore, a composite NCCV intensity index (NCCVI) was defined as a comprehensive measure of NCCV's central intensity and peripheral influence area. The expression is as follows:

$$\mathrm{NCCVI}=\overline{\left[\frac{\iint \mathrm{CVI}\,\mathrm{d}A}{\iint \mathrm{d}A}\right]},$$

$$\mathrm{CVI}=\begin{cases}\mathrm{vor}_{850}, \text{within a cyclone}\\ 0, \text{outside a cyclone}\end{cases}.$$

The over line in the expression denotes the summer average, and $\iint \mathrm{d}A$ indicates the area integration of NEC. vor_{850} indicates the values of relative vorticity at 850 hPa. The intensity of cold vortex (CVI) only accounts for the area inside NEC. Compared to those considering only the intensity at the center of NCCV, this NCCV intensity definition can provide a more composite representation of the overall NCCV, especially for its peripheral influence area. Then, the summer average NCCVI was calculated and normalized, and when referring to NCCVI in the subsequent text, it denotes the normalized NCCVI in summer.

3 RESULTS

3.1 *Climatological characteristics of NCCVs in summer*

Statistics on summer cyclones in East Asia found that cyclones occur most frequently in the Mongolian Plateau, Daxinganling and NEC with a maximum frequency of up to 27% (see Fig. 1), suggesting that NCCVs may have potential impacts on the weather and climate of NEC and its surroundings in summer. Therefore, NEC, which is located in the downstream of the Mongolian Plateau, was selected as the main study area.

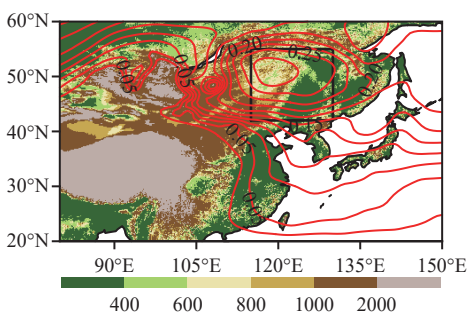

Figure 1. The 2D frequency (units: %) of extratropical cyclones in East Asia from 1979 to 2018 in summer (contours). The shaded indicates the terrain elevation (units: m), and the black box represents Northeastern China.

From the normalized time series of summer NCCVI (Fig. 2a), it can be seen that NCCV activities exhibited a significant inter-annual variability, but there was no significant trend (–0.22±0.25 per decade). Statistically, the amplitudes of the summer NCCVI in 21 years exceeded one standard deviation (1 STD), i.e., anomalous years (red and blue dots in Fig. 2a). Specifically, the NCCVI indexes were greater than 1 STD in 1981, 1983, 1984, 1987, 1990, 1998, 2003, 2009 and 2013 (i.e., nine strong years), while the NCCVI indexes in 1980, 1982, 1988, 1994, 1999, 2001, 2002, 2004, 2008, 2010, 2011 and 2014 (i.e., 12 weak years) were less than 1 STD, suggesting a large inter-annual difference. Moreover, the results of power spectrum analysis (Fig. 2b) indicate that the summer NCCV activities had an obvious periodicity of 3–4 years and 6–7 years.

3.2 *Atmospheric circulation of summer NCCVs in anomalous years*

The atmospheric circulation of summer NCCVs in anomalous years was further investigated by the comparison of several meteorological elements between the strong and weak NCCVI years. Fig. 3 shows the composite differences of the 300 hPa, 500 hPa, and 850 hPa geopotential height fields in the strong and weak NCCVI years. Compared with the weak NCCVI years, the geopotential height fields in the strong NCCVI years showed obvious negative anomalies in the entire troposphere above NEC, suggesting a clear quasi-barotropic structure. In contrast, there were obvious positive anomalies of geopotential height in the entire troposphere over the Ural Mountains. The coupling of geopotential height anomalies between the Ural Mountains and NEC together led to an increase in the zonal gradient of the geopotential height between them. It was prone to trigger anomalous northeasterly winds according to the geostrophic wind principle. On the contrary, the opposite geopotential height anomalies between NEC and the

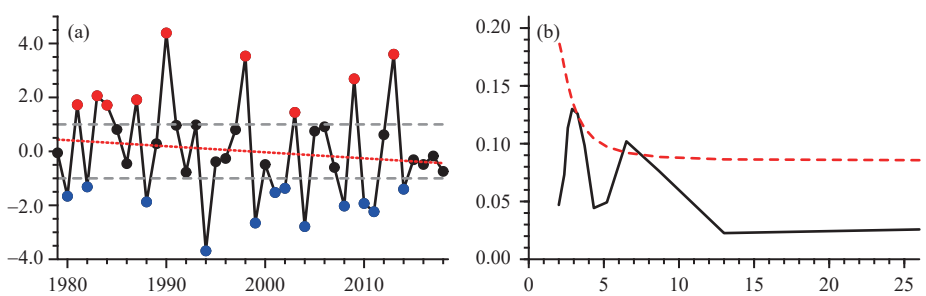

Figure 2. (a) The normalized time series of summer NCCVI from 1979 to 2018, and (b) its power spectrum analysis. The gray and red dashed lines in Fig. 2a indicate ±1 standard deviation, and the linear regression of NCCVI fitted by least squares; the red (blue) dots represent strong (weak) anomalous years, respectively. The black line in Fig. 2b indicates the smoothed spectrum estimate values, and the red dashed line represents the red noise standard spectrum is statistically significant at the confidence level of 90%.

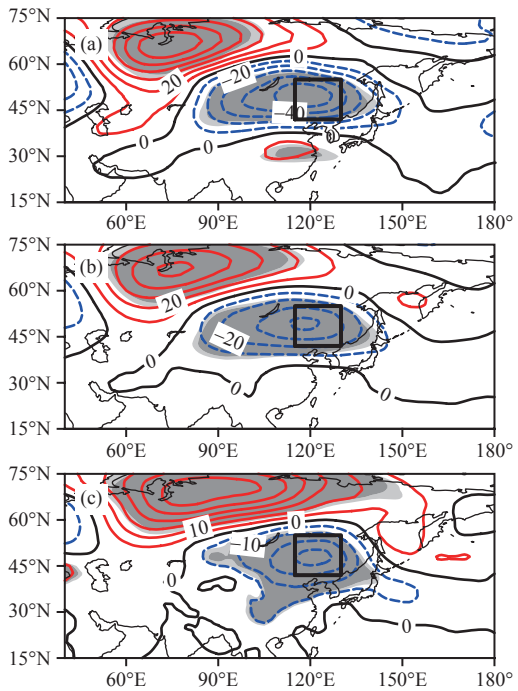

Figure 3. The composite differences of geopotential height fields (contours, units: gpm) at (a) 300 hPa, (b) 500 hPa, and (c) 850 hPa between strong and weak NCCVI years. The light (dark) gray shaded area indicates results statistically significant at the confidence level of 90% (95%). The black boxes indicate Northeastern China.

middle and low reaches of the Yangtze River promoted the occurrence of anomalous westerly winds. Then, an anomalous cyclonic circulation was favorable for the maintenance and strengthening of NCCV activities.

The composite differences of horizontal winds are shown in Fig. 4; it is found that there were obvious northeasterly anomalies between the Ural Mountains and NEC, which was roughly located between the centers of positive and negative anomalies of the geopotential height. An anti-cyclonic circulation anomaly appeared over the Ural Mountains, with a cyclonic circulation anomaly above NEC, which coincided with the geopotential height field. Moreover, the wind anomalies at 300 hPa were significantly stronger than those at 850 hPa, indicating that there was an obvious vertical wind shear near NEC, which was conducive to the enhancement of baroclinicity and provided favorable conditions for the enhancement and maintenance of NCCV activities.

The composite differences of temperature in the lower troposphere are given in Fig. 5. It can be observed that in the strong NCCVI years, there were significant negative temperature anomalies in the lower troposphere in NEC, while there were positive temperature anomalies in the Ural Mountains. The temperature anomaly value of the cold center was <–1.5°C, while the temperature anomaly value of the warm center was >1.5°C. The temperature anomalies in the lower troposphere satisfied the principle of thermal wind, which was the main reason for the significant vertical wind shear between the Ural Mountains and NEC.

Moreover, the negative temperature anomalies in NEC promoted the loss of atmospheric column mass due to the cooling contraction of the air column. This was accompanied by negative geopotential height and cyclonic circulation anomalies, providing a favorable local atmospheric condition for the development of NCCV activity. Furthermore, NCCV is generally considered a product of large-scale circulation patterns under specific conditions in NEC. Its activity interacts with blocking highs in a mutually reinforcing manner. Therefore, the

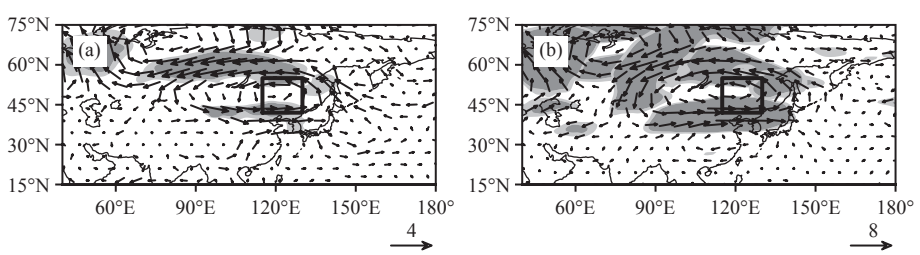

Figure 4. The composite differences of horizontal winds (vectors, units: m s^{-1}) at (a) 850 hPa and (b) 300 hPa between strong NCCVI years and weak NCCVI years. The light (dark) gray shaded area indicates results statistically significant at the confidence level of 90% (95%). The black boxes indicate Northeastern China.

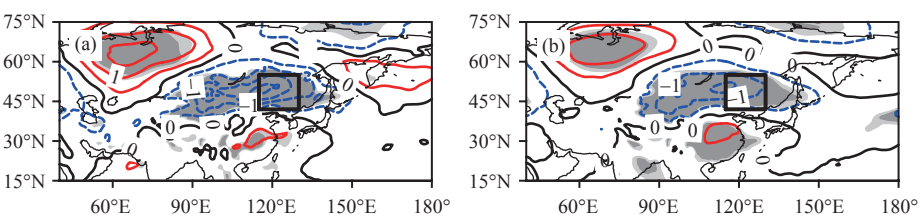

Figure 5. The composite differences of temperature (contours, units: °C) at (a) 850 hPa and (b) 700 hPa between strong and weak NCCVI years. The light (dark) gray shaded area indicates results statistically significant at the confidence level of 90% (95%). The black boxes indicate Northeastern China.

circulation of positive geopotential height anomalies over the Ural Mountains also favored the formation of NCCV (Zhang et al. [1]).

3.3 *Linkage between summer NCCV activities and simultaneous precipitation*

From the above analyses of the atmospheric circulation in anomalous NCCVI years, we may find that the fields of geopotential height, wind and temperature in NEC and its vicinity cooperated closely with each other and form a circulation background, which was conducive to the maintenance and development of NCCV activities. To explore the connection between the summer NCCV activities and the contemporaneous precipitation in China, the correlation analysis of NCCVI and precipitation was calculated by using data from Chinese meteorological stations as well as the ERA-Interim reanalysis dataset. As shown in Fig. 6a, there was a significant positive correlation between the NCCVI and the contemporaneous precipitation in NEC, and the correlation coefficients in most areas of NEC were higher than 0.4, with the maximum value reaching 0.6. The results calculated with the reanalysis dataset also showed a significant positive correlation there, with relatively higher correlation coefficients (Fig. 6b). This indicates that when the summer NCCV activities were anomalously stronger, the contemporaneous precipitation in NEC increased significantly.

Moreover, Fig. 6c shows that there was also a good negative correlation between the NCCVI and summer surface temperature in NEC, either in the Chinese meteorological station data or the ERA-Interim reanalysis dataset. The correlation coefficients in most areas of NEC were lower than –0.4, and the minimum value could reach –0.6. This indicates that the summer surface temperature in NEC was significantly lower during strong NCCVI years. Furthermore, the results of Chinese meteorological station data and the ERA-Interim reanalysis dataset consistently show that there was a significant positive correlation between NCCVI and surface temperature in South China and the Yangtze River.

Meanwhile, the scatter diagram of the NCCVI and regional average precipitation (surface temperature) in NEC (Fig. 7) also shows a significant positive (negative) correlation between NCCVI and precipitation (surface temperature). The correlation coefficient between NCCVI and the regional average of precipitation (surface temperature) in NEC was 0.52 (–0.33), which was statistically significant at the confidence level of 95%. That is, in strong NCCVI years, the summer precipitation increased in NEC with lower surface temperatures. In weak NCCVI years, the situation was the opposite.

Based on the statistics of total precipitation contribution in summer, it is found that precipitation associated with NCCV activities constituted approximately 58.5% of the total precipitation in NEC, which emphasized the important role of NCCV as one of the major precipitation systems in NEC. Moreover, the composite difference in surface temperature between periods of NCCV presence and absence reveals that when NCCV activity occurred, the surface temperature in NEC was significantly lower, with a regional average temperature difference of –0.95 K (statistically significant at the confidence level of 90%).

To further show the climatic effects of NCCV, the integrated water vapor flux and its divergence are given in Fig. 8a. From which it can be seen that during the strong NCCVI years, a large amount of water vapor converged in NEC due to the anomalous NCCV activities, which was mainly from two water vapor transportation belts. One of the belts was located on the southeast side of NEC, and water vapor from the downstream of the Yangtze River flowed into NEC through this belt associated with the East Asian summer monsoon. Another belt was located on the

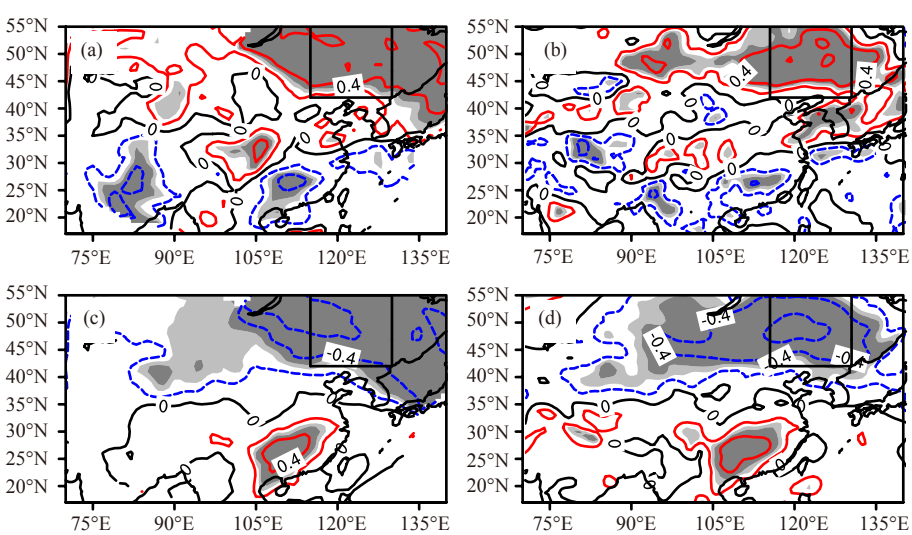

Figure 6. The correlation coefficient between NCCVI and monthly total precipitation was calculated from (a) Chinese meteorological station data and (b) the ERA-Interim reanalysis dataset. (c, d) are similar to (a, b), but for the correlation between NCCVI and monthly mean temperature at 2m. (c) is based on data from Chinese meteorological stations, and (d) is based on the ERA-Interim reanalysis dataset. The light (dark) gray shaded area indicates results statistically significant at the confidence level of 90% (95%). The black boxes indicate Northeastern China.

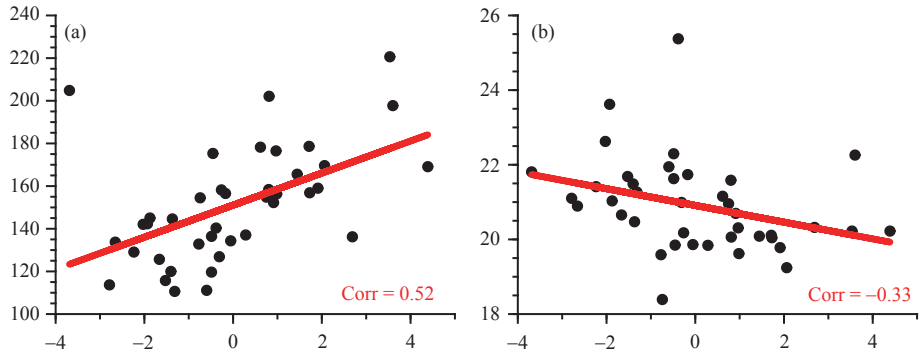

Figure 7. (a) The scatter diagram of summer NCCVI (*x*-axis) and regional average monthly total precipitation (*y*-axis) in Northeastern China. (b) is similar to (a), but for the scatter diagram of summer NCCVI (*x*-axis) and regional average monthly surface temperature at 2 m (*y*-axis). The red lines indicate linear regressions of NCCVI on precipitation and surface temperature, respectively. The correlation coefficients between NCCVI and the regional average of precipitation or surface temperature are 0.52 and –0.33, respectively; the results are both statistically significant at the confidence level of 95%.

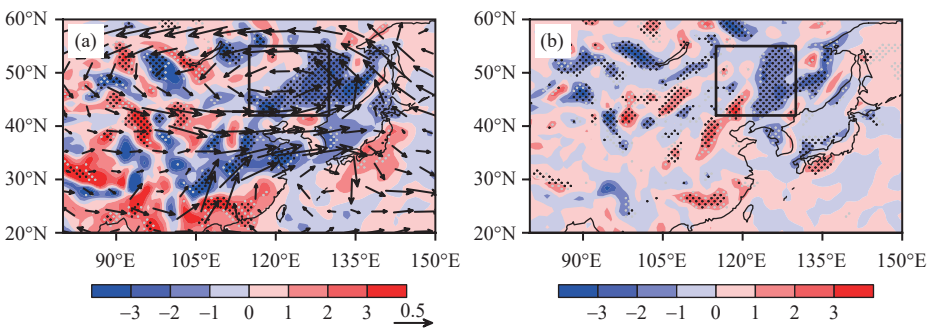

Figure 8. The composite differences of (a) integrated water vapor flux (vectors, units: 10^2 kg m^{-1} s^{-1}) and its divergence (shaded, units: 10^{-5} kg m^{-2} s^{-1}), as well as (b) vertical velocity (shaded, units: 10^{-2} Pa s^{-1}) at 850 hPa between strong and weak NCCVI years. The gray (black) dots indicate results statistically significant at the confidence level of 90% (95%). The black boxes indicate Northeastern China.

east side of NEC, transporting the water vapor from the Northwestern Pacific into NEC. Furthermore, under the influence of NCCV activities, there was a significant anomalous upward motion in the lower troposphere (Fig. 8b). Increased water vapor and upward motion both provided favorable conditions for potential precipitation in NEC.

3.4 *Possible mechanisms impacting the summer NCCV activities*

As mentioned above, favorable atmospheric circulation occurred in NEC during strong NCCVI years, accompanied by coupled circulation in the Ural Mountains, and there was a significant positive correlation between NCCVI and precipitation in NEC. To further understand the intensification mechanisms of NCCV activities in summer, we explored the linkage between NCCVI and the contemporaneous SST of the North Atlantic (Fig. 9). It can be observed that there was a significant positive correlation between them. The correlation coefficient can reach up to about 0.3 in the mid-latitude Atlantic. Furthermore, the regression of geopotential height fields at different levels on the NCCVI are given in Fig. 10; it is found that there existed a wave-train-like anomalous geopotential height in the troposphere from the mid-latitude Atlantic to NEC via western Europe and Ural Mountains. The circulation characteristics near the Ural Mountains and NEC were similar to the composite analysis results of geopotential height (Fig. 3). This implies that anomalous Rossby waves were excited in the Atlantic and propagate eastward, which finally affected NEC. Many previous studies have also emphasized the importance of the similar Rossby wave train propagating from the Northern Atlantic to East Asia, such as the East Atlantic/West Russia teleconnection pattern (Barnston and Livezey [30]; Lim [31]), Scandinavia teleconnection pattern (Wallace and Gutzler [32]; Bueh and Nakamura [33]), British-Baikal Corridor teleconnection pattern (Xu et al. [34]), as well as Silk Road teleconnection pattern (Lu et al. [35]; Wang et al. [36]).

The regressions of the surface sensible heat and latent heat flux fields on NCCVI are given in Fig. 11. As a result of the Atlantic SST heat anomalies, large amounts of surface sensible and latent heat flux were transported into the lower troposphere. Based on the composite analysis of the vertical circulation (Fig. 12) and the surface thermal characteristics over the Atlantic, it is found that as the Atlantic SST rose, the geopotential height increased in its vicinity and a positive geopotential height anomaly occurred in the east side of its heat source. Moreover, it was accompanied by an anomalous upward motion, which formed an anomalous thermal circulation (Fig. 12). As a result, an eastward diverging flow was formed in the upper troposphere and propagates downstream.

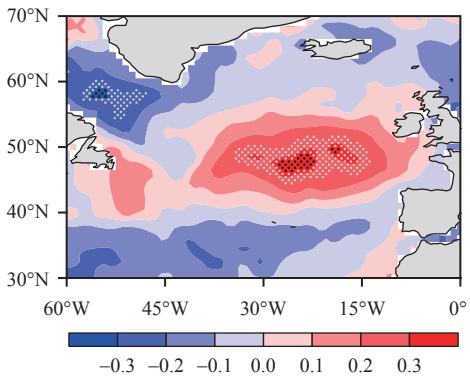

Figure 9. The correlation of NCCVI and SST of the Atlantic. The gray (black) dots indicate results statistically significant at the confidence level of 95%.

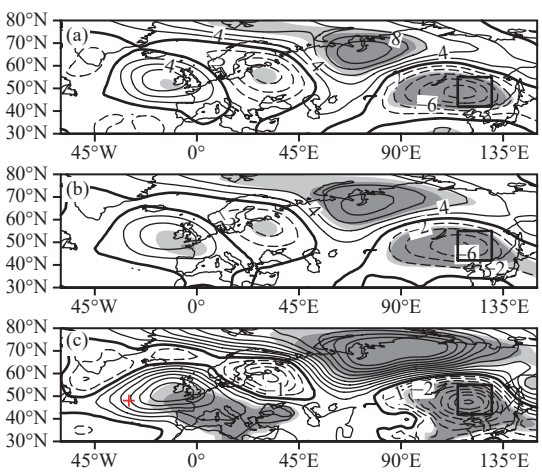

Figure 10. The regression of geopotential height fields (contours, units: gpm) at (a) 300 hPa, (b) 500 hPa, and (c) 850 hPa on NCCVI. The "+" symbol in (c) indicates the location of the SST warm anomaly center. The light (dark) gray shaded area indicates results statistically significant at the confidence level of 90% (95%), and the black boxes indicate Northeastern China.

This phenomenon is inseparably linked to the propagation of the Rossby wave train. The horizontal T-N wave activity fluxes (Takaya and Nakamura [37]) are an effective diagnostic of Rossby wave activity, and their expression is as follows:

$$W=\frac{p\cos\varphi}{2|\boldsymbol{U}|}\cdot$$

$$\begin{pmatrix}\dfrac{U}{a^2\cos^2\varphi}\left[\left(\dfrac{\partial\psi'}{\partial\lambda}\right)^2-\psi'\dfrac{\partial^2\psi'}{\partial\lambda^2}\right]+\dfrac{V}{a^2\cos\varphi}\left[\dfrac{\partial\psi'}{\partial\lambda}\dfrac{\partial\psi'}{\partial\varphi}-\psi'\dfrac{\partial^2\psi'}{\partial\lambda\partial\varphi}\right]\\ \dfrac{U}{a^2\cos\varphi}\left[\dfrac{\partial\psi'}{\partial\lambda}\dfrac{\partial\psi'}{\partial\varphi}-\psi'\dfrac{\partial^2\psi'}{\partial\lambda\partial\varphi}\right]+\dfrac{V}{a^2}\left[\left(\dfrac{\partial\psi'}{\partial\varphi}\right)^2-\psi'\dfrac{\partial^2\psi'}{\partial\varphi^2}\right]\end{pmatrix}$$

where $\boldsymbol{U}$ indicates the climatological horizontal wind vectors in summer, including zonal component U and meridional component V, $\psi'=\dfrac{\varphi'}{f}$ indicates stream function anomalies, and p, φ, λ, and a indicate basic meteorological parameters respectively. Based on the regression of horizontal T-N wave activity fluxes on NCCVI (Fig. 13), it is evident that a clear Rossby wave train propagated eastward from the Atlantic via western Europe and the Ural Mountains, eventually affecting NEC.

4 CONCLUSION

This paper employed an automatic algorithm to identify the summer extratropical cyclones in NEC (i.e., NCCVs) from 1979 to 2018. Based on a defined NCCV intensity index (NCCVI), the atmospheric circulation in NEC between strong and weak NCCVI years and its relationship with the contemporaneous precipitation and temperature were further explored. Moreover, the potential development mechanisms of NCCV activities were also investigated. The main findings are summarized as follows:

(1) The NCCV activities in summer exhibited a strong inter-annual variability, with an obvious periodicity of 6–7 years, but without a significant trend. During the strong NCCVI years, there were negative geopotential height anomalies in NEC, accompanied by cyclonic circulation and negative temperature anomalies, which were conducive to the maintenance and development of NCCV activities. The atmospheric circulation was opposite in the Ural Mountains.

(2) The NCCVI had a significant positive correlation with the summer precipitation in NEC, as well as a significant negative correlation with surface temperature in summer. Large amounts of water vapor converged in NEC from the downstream of the Yangtze River and Northwestern Pacific during the strong NCCVI years through two water vapor transportation belts, and there was a significant anomalous upward motion in the lower troposphere over NEC.

(3) The NCCV activities in summer were associated with the anomalous SST of the Atlantic. As the Atlantic SST rose, large amounts of surface sensible and latent heat flux were thus transported into the lower troposphere. This associated external heating triggered a mid-latitude eastward propagating Rossby wave train in the upper troposphere, which led to a coupled circulation in the Ural Mountains and NEC, as well as the more intensive NCCV activities in summer.

The NCCV is typically accompanied by heavy rain, hail, thunderstorms, strong winds, and low-temperature freezing (Zhang et al. [1]; He et al. [2]). NCCV activities are closely related to the precipitation not only in NEC but also in East Asia, profoundly affecting the agricultural development and socio-economy of the local area and East Asia. Investigating the behaviors of NCCV and its intensification mechanisms has a significant impact on clarifying the climate variability in East Asia and is an important indicator for precipitation and temperature climate forecasting in China, especially the prediction of heavy precipitation and extreme freezing hazards. However, due to the complexity of factors influencing extreme climate events, a more in-depth exploration is still necessary for a quantitative analysis of the impact of NCCV on the local climatic anomaly, as well as numerical simulations of the driven role of SST/SSTA in the North Atlantic on NCCV activities.

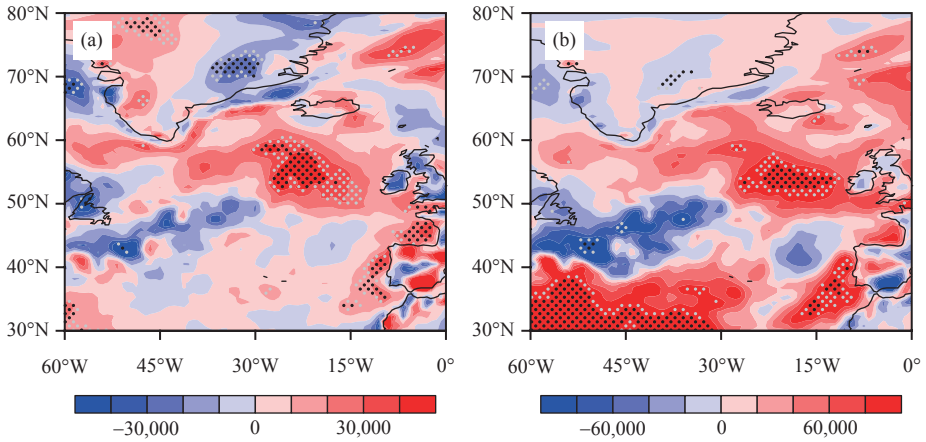

Figure 11. The regressions of (a) surface sensible heat flux (units: J m^{-2}) and (b) surface latent heat flux (units: J m^{-2}) on NCCVI. The gray (black) dots indicate results statistically significant at the confidence level of 90% (95%).

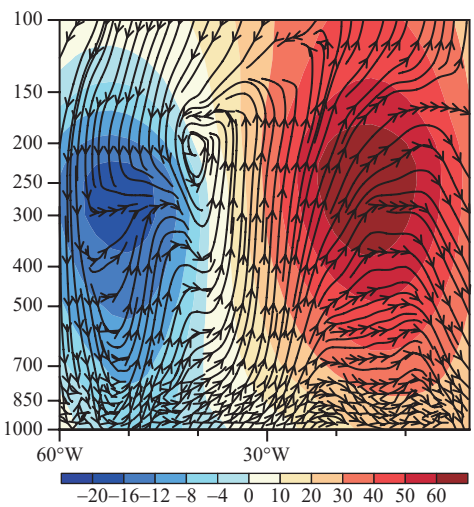

Figure 12. The regression of 50°–60°N meridional averaged profile of *u*-*w* winds (streamline) and geopotential height (shaded, units: gpm) on NCCVI.

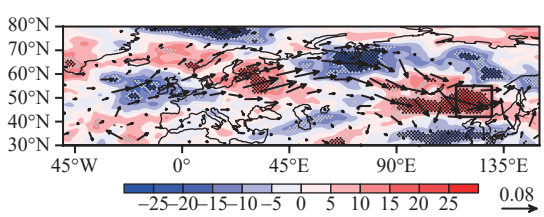

Figure 13. The regression of horizontal T-N wave activity fluxes (vectors, units: m^2 s^{-2}) and relative vorticity (shaded, units: 10^{-7} s^{-1}) at 300 hPa on NCCVI. The gray (black) dots indicate results statistically significant at the confidence level of 90% (95%).

REFERENCES

[1] ZHANG Li-xiang, LI Ze-chun. A summary of research on cold vortex over Northeast China [J]. Climatic and Environmental Research, 2009, 14(2): 218—228, in Chinese with English abstract

[2] HE Jin-hai, WU Zhi-wei, QI Li, et al. Relationships among the Northern Hemisphere annual mode, the Northeast cold vortex and the summer rainfall in Northeast China [J]. Journal of Meteorology and Environment, 2006, 22(1): 1–5, in Chinese with English abstract

[3] HE Jin-hai, WU Zhi-wei, JIANG Zhi-hong, et al. "Climate effect" of the northeast cold vortex and its influences on Meiyu [J]. Chinese Science Bulletin, 2007, 52(5): 671–679, https://doi.org/10.1007/s11434-007-0053-z

[4] HU Kai-xin, LU Ri-yu, WANG Dong-hai. Seasonal climatology of cut-off lows and associated precipitation patterns over Northeast China [J]. Meteorology and Atmospheric Physics, 2010, 106(1–2): 37–48, https://doi.org/10.1007/s00703-009-0049-0

[5] NIETO R, GIMENO L, DE LA TORRE L, et al. Climatological features of cutoff low systems in the Northern Hemisphere [J]. Journal of Climate, 2005, 18 (16): 3085–3103, https://doi.org/10.1175/jcli3386.1

[6] ZHANG C, ZHANG Q, WANG Y, et al. Climatology of warm season cold vortices in East Asia: 1979–2005 [J]. Meteorology and Atmospheric Physics, 2008, 100(1–4): 291–301, https://doi.org/10.1007/s00703-008-0310-y

[7] AWAN N K, FORMAYER H. Cutoff low systems and their relevance to large-scale extreme precipitation in the European Alps [J]. Theoretical and Applied Climatology, 2017, 129(1–2): 149–158, https://doi.org/10.1007/s00704-016-1767-0

[8] WERNLI H, SCHWIERZ C. Surface cyclones in the ERA-40 Dataset (1958–2001), Part I: novel identification method and global climatology [J]. Journal of the Atmospheric Sciences, 2006, 63(10): 2486–2507, https://doi.org/10.1175/jas3766.1

[9] LU Chu-han. A modified algorithm for identifying and tracking extratropical cyclones [J]. Advances in Atmospheric Sciences, 2017, 34(7): 909–924, https://doi.org/10.1007/s00376-017-6231-2

[10] SUN Li, ZHENG Xiu-ya, WANG Qi. The climatological characteristics of northeast cold vortex in China [J]. Quarterly Journal of Applied Meteorology, 1994, 5(3): 297–303, in Chinese with English abstract

[11] XIE Z W, BUEH C. Low frequency characteristics of northeast China cold vortex and its background circulation pattern [J]. Acta Meteorologica Sinica, 2012, 70(4): 704–716, in Chinese with English abstract

[12] LIU Gang, LIAN Yi, YAN Peng-cheng, et al. The objective recognition and classification of Northeast cold vortex and the Northern Hemisphere atmospheric circulation characters in May to August [J]. Scientia Geographica Sinica, 2015, 35(8): 1042–1050, in Chinese with English abstract

[13] LIAN Yi, BUEH C, XIE Zuo-wei, et al. The anomalous cold vortex activity in Northeast China during the early

summer and the low-frequency variability of the northern hemispheric atmosphere circulation [J]. Chinese Journal of Atmospheric Sciences, 2010, 34(2): 429–439, in Chinese with English abstract

[14] LIANG Hong, WANG Yuan, GUO Zheng-qiang. The teleconnection relationship between the Northeast cold vortex and the subtropical high, the Okhotsk high in summer [J]. Journal of the Meteorological Sciences, 2009, 29(6): 793–796, in Chinese with English abstract

[15] LIU Ying, WANG Dong-hai, ZHANG Zhong-feng, et al. A comprehensive analysis of the structure of a Northeast China cold vortex and its characteristics of evolution [J]. Acta Meteorologica Sinica, 2012, 70(3): 354–370, in Chinese with English abstract

[16] GAO Hui, GAO Jing. Increased influences of the SST along the Kuroshio in previous winter on the summer precipitation in Northeastern China [J]. Acta Oceanologica Sinica, 2014, 36(7): 27–33, in Chinese with English abstract

[17] ZHANG Jiu-zheng, XU Hai-ming, MA Jing, et al. Interannual variability of spring extratropical cyclones over the Yellow, Bohai, and East China Seas and possible causes [J]. Atmosphere, 2019, 10(1): 40, https://doi.org/10.3390/atmos10010040

[18] ZHANG Qing-yun, TAO Shi-yan. Influence of Asian mid-high latitude circulation on East Asian summer rainfall [J]. Acta Meteorologica sinica, 1998, 56(2): 72–84, in Chinese with English abstract

[19] ZHAO Si-xiong, SUN Jian-hua. Study on cut-off low-pressure systems with floods over Northeast Asia [J]. Meteorology and Atmospheric Physics, 2007, 96(1–2): 159–180, https://doi.org/10.1007/s00703-006-0226-3

[20] XIE Z W, BUEH C. Different types of cold vortex circulations over Northeast China and their weather impacts [J]. Monthly Weather Review, 2015, 143(3): 845–863, https://doi.org/10.1175/MWR-D-14-00192.1

[21] DING Shi-sheng. The climatic analysis of low temperature in summer over Northeast China and influence for agricultural product [J]. Acta Meteorologica Sinica, 1980, 38(3): 234–242, in Chinese with English abstract

[22] LIU Hui-bin, WEN Min, HE Jin-hai, et al. Characteristics of the Northeast cold vortex at intraseasonal timescale and its impact [J]. Chinese Journal of Atmospheric Sciences, 2012, 36(5): 959–973, in Chinese with English abstract

[23] LU Chu-han, KONG Yang, LI Kai-li, et al. The impacts of winter snow cover of central Asia on the Northeastern China cold vortex in succeeding spring [J]. Climate Dynamics, 2024, 1–13, https://doi.org/10.1007/s00382-023-07075-0

[24] MIAO Chun-sheng, WU Zhi-wei, HE Jin-hai, et al. The anomalous features of the Northeast Cold Vortex during the first flood period in the last 50 years and its correlation with rainfall in South China [J]. Chinese Journal of Atmospheric Sciences, 2006, 30(6): 1249–1256, in Chinese with English abstract

[25] YANG Han-wei, FENG Guo-lin, SHEN Bai-zhu, et al. The quantitative research on cold vortex in summer over Northeast China [J]. Chinese Journal of Atmospheric Sciences, 2012, 36(3): 487–494, in Chinese with English abstract

[26] ECMWF ERA-interim Project [Z]. NCAR: Research Data Archieve, 2009, https://doi.org/10.5065/D6CR5RD9

[27] DEE D, UPPALA S, SIMMONS A, et al. The ERA-Interim reanalysis: configuration and performance of the data assimilation system [J]. Quarterly Journal of the Royal Meteorological Society, 2011, 137(656): 553–597, https://doi.org/10.1002/qj.828

[28] Hadley Centre for Climate Prediction and Research/Met Office/Ministry of Defence/United Kingdom. Hadley Centre Global Sea Ice and Sea Surface Temperature (HadISST) (Updated monthly) [Z]. Research Data Archive at the National Center for Atmospheric Research, Computational and Information Systems Laboratory, 2000, https://doi.org/10.5065/XMYE-AN84

[29] NEU U, AKPEROV M, BELLENBAUM N, et al. IMILAST: a community effort to intercompare extratropical cyclone detection and tracking algorithms [J]. Bulletin of the American Meteorological Society, 2013, 94(4): 529–547, https://doi.org/10.1175/bams-d-11-00154.1

[30] BARNSTON A G, LIVEZEY R E. Classification, seasonality and persistence of low-frequency atmospheric circulation patterns [J]. Monthly Weather Review, 1987, 115(6): 1083–1126, https://doi.org/10.1175/1520-0493(1987)115<1083:CSAPOL>2.0.CO;2

[31] LIM Young-kwon. The East Atlantic/West Russia (EA/WR) teleconnection in the North Atlantic: climate impact and relation to Rossby wave propagation [J]. Climate Dynamics, 2015, 44(11–12): 3211–3222, https://doi.org/10.1007/s00382-014-2381-4

[32] WALLACE J M, GUTZLER D S. Teleconnections in the geopotential height field during the Northern Hemisphere winter [J]. Monthly Weather Review, 1981, 109(4): 784–812, https://doi.org/10.1175/1520-0493(1981)109<0784:TITGHF>2.0.CO;2

[33] BUEH C, NAKAMURA H. Scandinavian pattern and its climatic impact [J]. Quarterly Journal of the Royal Meteorological Society, 2007, 133(629): 2117–2131, https://doi.org/10.1002/qj.173

[34] XU Pei-qiang, WANG Lin, CHEN Wen. The British-Baikal corridor: a teleconnection pattern along the summertime polar front jet over Eurasia [J]. Journal of Climate, 2019, 32 (3): 877–896, https://doi.org/10.1175/JCLI-D-19-0458.1

[35] LU R Y, OH J H, KIM B J. A teleconnection pattern in upper-level meridional wind over the North African and Eurasian continent in summer [J]. Tellus A: Dynamic Meteorology and Oceanography, 2002, 54(1): 44–55, https://doi.org/10.3402/tellusa.v54i1.12122

[36] WANG L, XU P, CHEN W, et al. Interdecadal variations of the Silk Road pattern [J]. Journal of Climate, 2017, 30(24): 9915–9932, https://doi.org/10.1175/JCLI-D-17-0340.1

[37] TAKAYA K, NAKAMURA H. A formulation of a phase-independent wave-activity flux for stationary and migratory quasigeostrophic eddies on a zonally varying basic flow [J]. Journal of the Atmospheric Sciences, 2001, 58(6): 608–627, https://doi.org/10.1175/1520-0469(2001)058<0608:AFOAPI>2.0.CO;2

Citation: KONG Yang, LU Chu-han, LI Kai-li, et al. Analysis of Summer Cold Vortex Activity Anomalies in Northeastern China and Their Relationship with Regional Precipitation and Temperature [J]. Journal of Tropical Meteorology, 2024, 30(2): 180–188, https://doi.org/10.3724/j.1006-8775.2024.016